THE JOURNAL OF PHYSICAL CHEMISTRY A

Article

pubs.acs.org/JPCA

Conformation of Alkali Metal Ion−Benzo-12-Crown-4 Complexes Investigated by UV Photodissociation and UV−UV Hole-Burning Spectroscopy

Yoshiya Inokuchi,* Maki Nakatsuma, Motoki Kida, and Takayuki Ebata

Department of Chemistry, Graduate School of Science, Hiroshima University, Higashi-Hiroshima, Hiroshima 739-8526, Japan

Supporting Information

ABSTRACT: We measure UV photodissociation (UVPD) spectra of benzo-12-crown-4 (B12C4) complexes with alkali metal ions, M^+·B12C4 (M = Li, Na, K, Rb, and Cs), in the 36300−37600 cm^{-1} region. Thanks to the cooling of ions to ∼10 K, all the M^+·B12C4 complexes show sharp vibronic bands in this region. For UV−UV hole-burning (HB) spectroscopy, we first check if our experimental system works well by observing UV−UV HB spectra of the K^+ complex with benzo-18-crown-6 (B18C6), K^+·B18C6. In the UV−UV HB spectra of the K^+·B18C6 complex, gain signals are also observed; these are due to vibrationally hot K^+·B18C6 complex produced by the UV excitation of cold K^+·B18C6 complex. Then we apply UV−UV HB spectroscopy to the M^+·B12C4 complexes, and only one conformer is found for each complex except for the Li^+ complex, which has two conformers. The vibronic structure around the origin band of the UVPD spectra is quite similar for all the complexes, indicating close resemblance of the complex structure. The most stable structures calculated for the M^+·B12C4 (M = Li, Na, K, Rb, and Cs) complexes also have a similar conformation among them, which coincides with the UVPD results. In these conformers the metal ions are too big to be included in the B12C4 cavity, even for the Li^+ ion. In solution, it was reported that 12-crown-4 (12C4) shows the preference of Na^+ ion among alkali metal ions. From the similarity of the structure for the M^+·B12C4 complexes, it is suggested that the solvation of free metal ions, not of the M^+·12C4 complexes, may lead to the selectivity of Na^+ ion for 12C4 in solution.

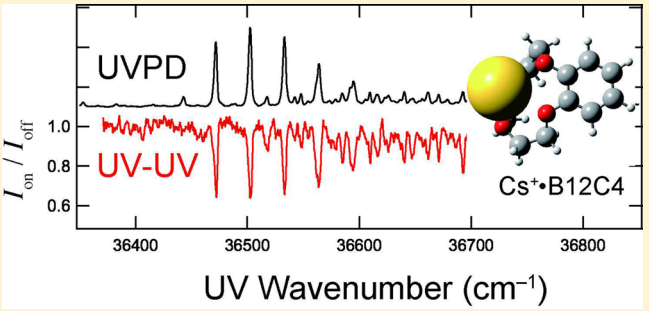

1. INTRODUCTION

Crown ethers (CEs) have been widely used as host molecules in host−guest, supramolecular, and organic chemistry; CEs can hold neutral or ion guests inside the cavity and transport or separate them.[1,2] One of the characteristics of CEs is the ion selectivity in solution. For instance, dibenzo-18-crown-6 (DB18C6) captures K^+ ion selectively among alkali metal ions in solution.[3] One explanation of the ion selectivity of CEs is the matching in size between the CE cavity and a guest ion.

Determination of the structure for guest ion−CE complexes has been extensively done by X-ray diffraction analysis of crystals. However, reports on X-ray diffraction analysis tend to be limited to optimum or selective systems. In the case of the M^+·DB18C6 complexes, there are 32 and 59 reports of X-ray analysis for M = Na and K, respectively, in the Cambridge Structural Database (CSD ver. 5.31) of the Cambridge Crystallographic Data Centre as of 2011.[4] However, there is no report for the Li^+·DB18C6, Rb^+·DB18C6, or Cs^+·DB18C6 1:1 complex; this is probably because these complexes cannot form stable crystals. To examine the origin of preferential capture of K^+ ion against other alkali metal ions, it would be necessary to study the structure of the M^+·DB18C6 complexes not only for M = K but also for other alkali metal ions. In addition, the main difference among the 59 crystal data of K^+·DB18C6 is counteranions or researchers reporting them, and the conformation of K^+·DB18C6 itself is almost the same for all the reports.

It is probable that effective capture of guest ions by CEs can originate from conformational flexibility, but the X-ray analysis hardly gives information on the flexibility of CEs and their effects to the ion selectivity. From this standpoint, gas-phase studies of CEs will play a vital role to shed light on the exact reason for the ion selectivity of CEs in solution.[5,6] Mass spectrometric studies have been reported for ion complexes of CEs since 1990s.[7−11] More recently, UV and IR spectroscopy have been performed for jet-cooled neutral CE complexes[12−21] and metal ion−CE complexes.[22−28] One of the advantages of gas-phase spectroscopy under cold conditions is the ability to measure conformer-specific spectra. This elucidates not only the structure of each conformer but also the number of conformations, which can provide the information on entropic effects to the complex formation; the larger the number of conformers is, the more favorable the complex formation is. It is difficult to obtain this information from condensed-phase

Received: July 1, 2016
Revised: July 26, 2016
Published: July 26, 2016

DOI: 10.1021/acs.jpca.6b06626
J. Phys. Chem. A 2016, 120, 6394−6401

spectroscopy or X-ray diffraction analysis. Kim and co-workers first reported UV photodissociation (UVPD) and UV−UV hole-burning (HB) spectra of metal ion−benzo-CE complexes under cold conditions.[29−33] We reported UVPD and IR−UV double-resonance (DR) spectra of metal ion complexes of DB18C6, benzo-18-crown-6 (B18C6), and benzo-15-crown-5 (B15C5) under colder conditions.[19,34−38] We also investigated UVPD, UV−UV HB, and IR−UV DR spectroscopy of CE complexes and pseudorotaxanes with H_2O^+, dibenzylamine·H^+, and aniline·H^+.[39,40]

In this paper, we extend our CE studies from 18-crown-6 (18C6) and 15-crown-5 (15C5) to a smaller one, that is, 12-crown-4 (12C4).[19,34−37,39] We measure UVPD spectra of benzo-12-crown-4 (B12C4, Figure 1) complexes with alkali

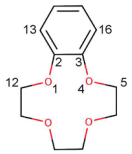

Figure 1. Atom numbering of B12C4.

metal ions, M^+·B12C4 (M = Li, Na, K, Rb, and Cs), under cold (∼10 K) conditions in the gas phase. We apply UV−UV HB spectroscopy to the M^+·B12C4 complexes to discriminate vibronic bands of a single conformer. The number and the structure of conformers are determined on the basis of these UVPD and UV−UV HB results with the aid of quantum chemical calculations. Finally we discuss the relation between the conformation of the M^+·B12C4 complexes and the ion preference of 12C4.

2. EXPERIMENTAL AND COMPUTATIONAL METHODS

Details of the experiment for UVPD spectroscopy have been described in our previous paper.[41] Briefly, the M^+·B12C4 complexes are produced by an electrospray ion source with methanol solutions of MCl salt and B12C4 with a concentration of ∼100 μM each. After passing through a vaporization tube (∼100 °C) and a skimmer, ions are introduced into the first octopole ion guide (OPIG). At the exit of the OPIG, a gate electrode is situated to bunch the continuous ion current. After the ion accumulation for ∼100 ms, the pulsed ion beam is ejected into the second OPIG and guided to a Paul-type quadrupole ion trap (QIT). The QIT is cooled to ∼4 K by a He cryostat, and He buffer gas is continuously introduced into the QIT. The ions are stored in the QIT for ∼90 ms and cooled translationally and internally by the collision with the cold He buffer gas. Ions other than parent ions of interest can be removed from the QIT by an RF potential applied to the entrance end-cap, as was done by Kang et al.[42] The parent ions are then irradiated by a UV laser, inducing the dissociation of the ions. After ∼1 μs of the UV excitation, resulting fragment ions are introduced to a homemade time-of-flight mass spectrometer and detected by a multichannel plate (MCP).[43] An output from the MCP is fed into a digital storage oscilloscope. Yields of the fragment ions are normalized by the intensity of the UV laser, and UVPD spectra of the parent ions are obtained by plotting normalized yields of the fragment ions against the wavenumber of the UV laser. The tunable UV light is obtained by second harmonic generation (SHG) of a fundamental output of a pulsed dye laser (Continuum ND6000) pumped by the third harmonics of a Nd:YAG laser (Continuum Surelite II), with a KDP crystal. A typical output energy of the UV laser used in this study is ∼0.5 mJ/pulse, and the repetition rate is 10 Hz.

In the UV−UV HB experiments, we use two laser systems. For the pump laser, we utilize the same system as that for UVPD spectroscopy described above, with a repetition rate of 5 Hz and an intensity of ∼0.5 mJ/pulse. For the probe light, we use the SHG of a fundamental output of a pulsed dye laser (Lambda Physik Scanmate) pumped by the third harmonics of a Nd:YAG laser (Continuum Surelite II), with a BBO crystal, and with an intensity of ∼0.1 mJ/pulse and a repetition rate of 10 Hz. The pump laser is introduced to the QIT prior to the probe one by 5−50 μs. In the experiments of the Na^+ and K^+ complexes, the photofragment metal ions produced by the pump laser are effectively removed from the QIT by the RF voltage applied to the ring electrode within ∼5 μs. For the Rb^+ and Cs^+ complexes, the fragment ions due to the pump laser are not sufficiently ejected by the RF potential. Hence, we apply an additional RF potential to the entrance end-cap of the QIT to remove the fragment ions.[42] The frequency of the additional RF potential is ∼100 kHz, and a longer delay (∼50 μs) is necessary for complete removal of the fragment ions due to the pump laser. The ion signal from the MCP is fed into and averaged by two oscilloscopes, which are triggered alternately with 5 Hz to monitor the fragment ion intensity only with the probe laser (I_{off}) and with the pump and probe laser (I_{on}). The wavenumber of the pump laser is scanned whereas that of the probe laser is fixed to a position of a vibronic band. The UV−UV HB spectra are obtained by plotting the ratio of the fragment ion intensity with the pump laser on/off (I_{on}/I_{off}) as a function of the wavenumber of the pump laser.

We also perform quantum chemical calculations for the M^+·B12C4 complexes. The initial conformation search is performed by using the CONFLEX High Performance Conformation Analysis program with the MMFF94s force field for the Li^+·B12C4, Na^+·B12C4, and K^+·B12C4 complexes.[38,44−46] The structure of the conformers obtained by the initial search are further optimized using the GAUSSIAN09 program package at the M05-2X/6-31+G(d) level of theory; at least 10 conformers are calculated for the M^+·B12C4 complexes each.[47] The vibrational analysis is also performed at the same calculation level. The transition energy and the oscillator strength are obtained theoretically by time-dependent density functional theory (TD-DFT) calculations at the M05-2X/6-31+G(d) level. For the Rb^+·B12C4 and Cs^+·B12C4 complexes, the initial structure for the geometry optimization with the GAUSSIAN09 is obtained by replacing the K^+ ion in the stable conformers of the K^+·B12C4 complex with Rb^+ or Cs^+ ion. For Rb and Cs, we use the Stuttgart RLC as effective core potentials (ECPs). Functions of the ECPs are obtained from a database of basis sets,[48] and they provided quite reasonable results in our previous papers of CE ion complexes.[34,35]

3. RESULTS AND DISCUSSION

3.1. UV Photodissociation Spectra. Figure 2 shows the UVPD spectra of the M^+·B12C4 (M = Li, Na, K, Rb, and Cs) complexes in the 36300−37600 cm^{-1} region. Thanks to the cooling of the ions in the QIT to ∼10 K,[41] all the complexes show sharp (∼3 cm^{-1} fwhm) and well-resolved vibronic bands. The UV spectra of M^+·B12C4 show a strong origin band at 36673, 36617, 36543, 36510, and 36472 cm^{-1} for M = Li, Na, K, Rb, and Cs, respectively. The existence of the strong origin band in each spectrum suggests rather small geometry change

DOI: 10.1021/acs.jpca.6b06626
J. Phys. Chem. A 2016, 120, 6394−6401

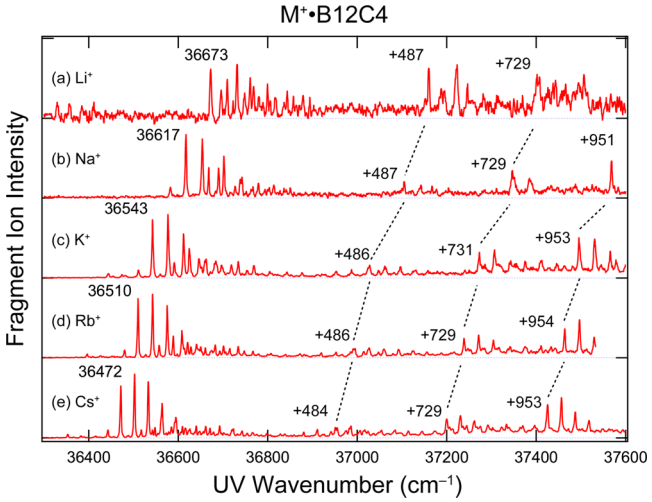

Figure 2. UVPD spectra of the M^+·B12C4 (M = Li, Na, K, Rb, and Cs) complexes.

upon the excitation from the S_0 to S_1 state for the M^+·B12C4 complexes, which is in contrast to the results that several conformers of the M^+·B15C5 and M^+·B18C6 complexes show a very weak origin band and substantially extended low-frequency progressions.[35] As shown with dotted lines in Figure 2, these complexes have vibronic bands at ~487, ~729, and ~953 cm^{-1} above the origin band; these bands can be assigned to the vibrations of the benzene ring (mode 6, 1, and 12, respectively), similar to the case of the M^+·DB18C6 complexes.[34] The Li^+ spectrum (Figure 2a) has a signal-to-noise ratio less than that of other complexes, because the photodissociation efficiency is much lower than the others. The vibronic bands of the Li^+ complex above 37100 cm^{-1} are more intense than those of the other complexes. This is probably because the photodissociation efficiency increases rapidly with increasing the UV frequency for the Li^+ complex.

3.2. UV–UV Hole-Burning Spectra. *3.2.1. K^+·B18C6 Complex.* The UV–UV HB spectra enable us to discriminate vibronic bands due to a single conformer. First we check if our HB measurement system works well by observing UV–UV HB spectra of the K^+·B18C6 complex. We reported that there are two conformers for K^+·B18C6 from the results of IR–UV DR spectroscopy,[35] and Kim and co-workers confirmed it by UV–UV HB spectroscopy.[33] Figure 3 shows the UV–UV HB spectra of the K^+·B18C6 complex (red curves) and the UVPD spectrum (black curve) that is measured again with our QIT machine.[35] In the UVPD spectrum (Figure 3a), two strong bands are observed at 36101 and 36398 cm^{-1}, which are assigned to the origin band of isomers K-i and K-ii in our previous report.[35] The UV–UV HB spectra in Figure 3b,c are measured by probing the origin band of K-i and K-ii, respectively. These UV–UV HB spectra well discriminate the vibronic bands of the two conformers as shown with dotted lines in Figure 3; the HB spectra measured at the origin band of K-i and K-ii (Figure 3b,c) show the depletion in the 36100–36300 and 36350–36600 cm^{-1} regions, respectively. In the spectrum of Figure 3b, positive signals are also found in the 36400–36600 cm^{-1} region. These positions coincide with the bands of K-ii. Similarly, the UV–UV spectrum measured at the origin band of K-ii (Figure 3c) shows weak positive signals at the sharp vibronic bands of K-i.

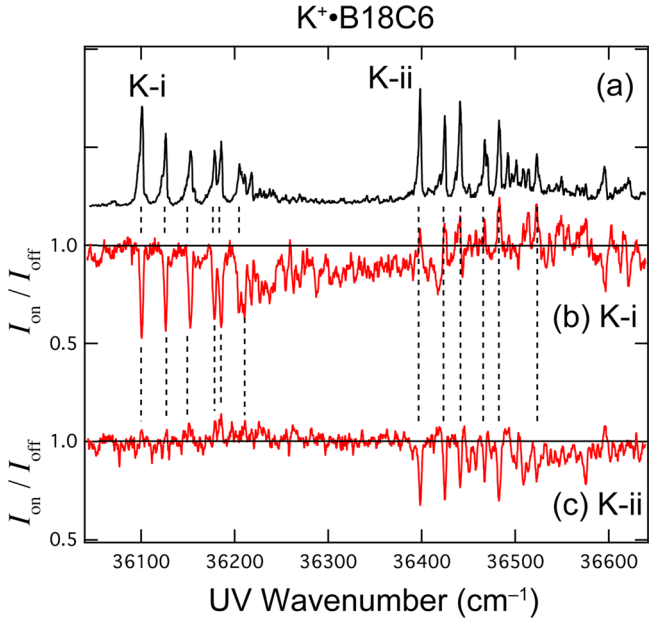

Figure 3. UV–UV HB spectra (red) and the UVPD spectrum (black) of the K^+·B18C6 complex. The HB spectra in (b) and (c) are measured by probing the origin band of K-i (36101 cm^{-1}) and K-ii (36398 cm^{-1}), respectively.

Figure 4 shows the UVPD spectrum (a) and UV–UV pump–probe spectra (b) of the K^+·B18C6 complex. The

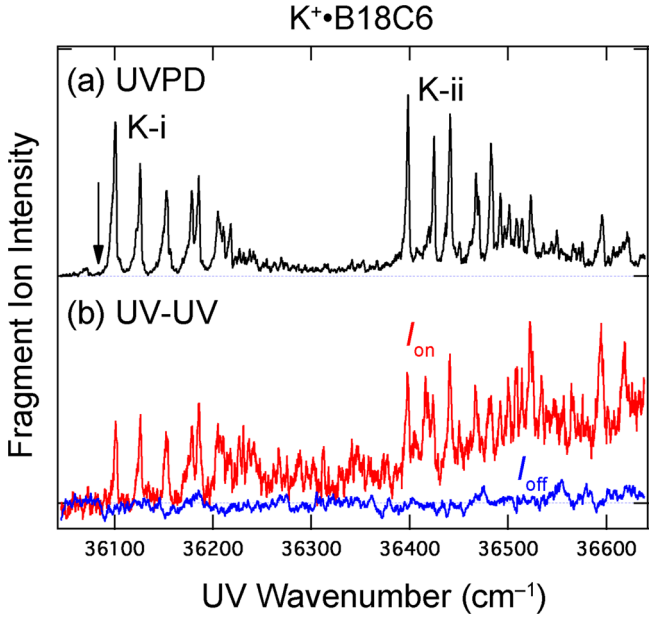

Figure 4. (a) UVPD spectrum of the K^+·B18C6 complex. (b) UV–UV pump–probe spectra of the K^+·B18C6 complex. These spectra are measured by scanning the pump frequency and fixing the probe frequency at a nonresonant position (36083 cm^{-1}). This position is shown with an arrow in Figure 4a.

pump–probe spectra are measured by fixing the probe wavenumber at a nonresonant position (36083 cm^{-1}); the position is shown by an arrow in Figure 4a. The UV–UV pump–probe spectrum (red curve in Figure 4b) shows sharp gain signals at the vibronic bands of K-i and K-ii. Therefore, we can ascribe the gain signals in Figures 3b,c and 4b to

DOI: 10.1021/acs.jpca.6b06626
J. Phys. Chem. A 2016, 120, 6394–6401

vibrationally hot K^+·B18C6 complex, which is produced by the photoexcitation of cold K-i and K-ii conformers and shows broad UV absorption. The delay between the pump and probe lasers was 5 μs for measuring the spectra in Figures 3b,c and 4b. The gain signals decrease with increasing delay time, with a lifetime of a few hundreds of microseconds. In our ion trap, the buffer He gas is continuously introduced. The above lifetime may correspond to the cooling of hot species by the collision with cold He gas. Examination of the formation and cooling processes of hot species in the UV−UV pump−probe scheme is our future work.

3.2.2. M^+·B12C4 Complexes. Then we apply UV−UV HB spectroscopy to the M^+·B12C4 complexes. Figure 5 displays

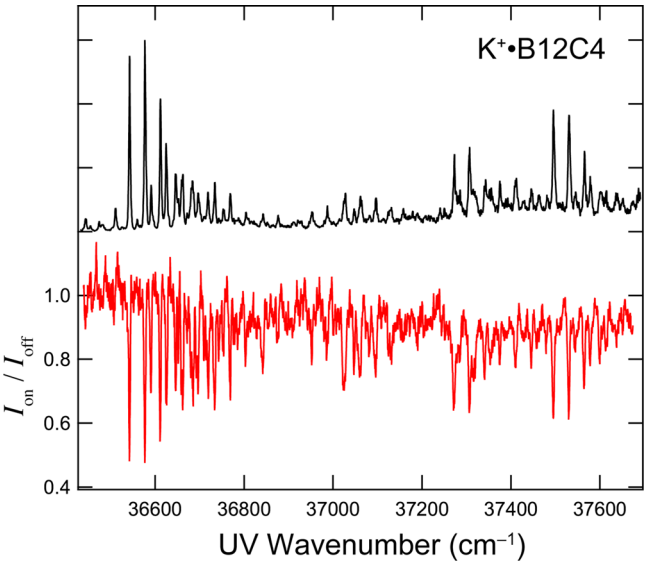

Figure 5. UV−UV HB spectrum (red) and the UVPD spectrum (black) of the K^+·B12C4 complex.

the UV−UV HB spectrum of the K^+·B12C4 complex (red curve) with the UVPD spectrum (black curve). For the UV−UV HB spectrum, the probe laser is fixed to the band origin at 36543 cm^{-1}, and the frequency of the pump laser is scanned. All the sharp bands in the UVPD spectrum appear also in the UV−UV HB spectrum, indicating that all the vibronic bands can be assigned to a single conformer. Figure 6 shows the UV−UV HB spectra (red curves) of the M^+·B12C4 (M = Na, K, Rb, and Cs) complexes observed by fixing the probe laser frequency at each origin band. Figure 6b is an expanded view of Figure 5 around the origin band. All the strong bands in the UVPD spectra emerge in the UV−UV HB spectra for all the ion complexes. Hence, the M^+·B12C4 (M = Na, K, Rb, and Cs) complexes each have only one conformation under the current cold conditions. For the Li^+·B12C4 complex, it is not possible to measure a UV−UV HB spectrum because of much weaker intensity of the fragment Li^+ ion.

Figure 7 shows expanded views of the UVPD spectra around the origin band. These spectra are plotted as a function of the UV wavenumber relative to the origin band. The vibronic structure is quite similar to each other, with a slight shift, as shown with dotted lines in Figure 7. In addition, the position of the origin band shifts to the red monotonously with increasing the ion size from Li^+ (36673 cm^{-1}) to Cs^+ (36472 cm^{-1}). Therefore, it is quite probable that all the conformers of M^+·B12C4 in the experiments have similar structures. On the

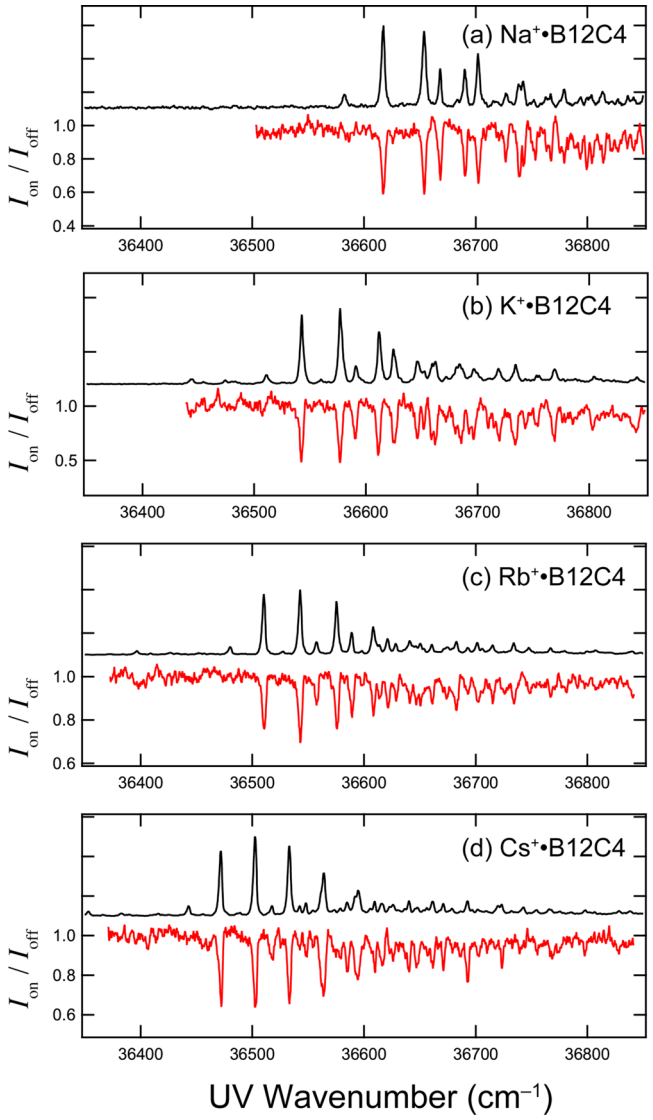

Figure 6. UV−UV HB spectra (red) and the UVPD spectra (black) of the M^+·B12C4 complexes.

contrary, for some of the vibronic bands of the Li^+ complex we cannot find corresponding bands in the spectra of the other complexes. These vibronic bands cannot be described starting from the band origin, so these bands should be assigned to different conformers. Because these bands show a regular interval of ∼35 cm^{-1}, as shown with solid lines in Figure 7a, those can be ascribed to a progression of a single conformer.

3.3. Conformations of the M^+·B12C4 Complexes. The experimental results described above are well explained with quantum chemical calculations. Figure 8 shows the most stable conformers of the M^+·B12C4 (M = Li, Na, K, Rb, and Cs) complexes calculated at the M05-2X/6-31+G(d) level. All the complexes in Figure 8 have quite similar conformations in the B12C4 part. The numbers in Figure 8 show the dihedral angles of C12−O1−C2−C13 and C16−C3−O4−C5 (Figure 1). The former angle ranges from 55° (Li^+) to 71° (Cs^+), but the latter one is almost the same for all the complexes (−32°). The difference in the total energy between the most and the second most stable conformers is more than 1 kJ/mol for all the M^+·B12C4 complexes: 1.2, 4.7, 4.8, 3.0, and 1.5 kJ/mol for M = Li, Na, K, Rb, and Cs, respectively. Therefore, the most abundant

DOI: 10.1021/acs.jpca.6b06626
J. Phys. Chem. A 2016, 120, 6394−6401

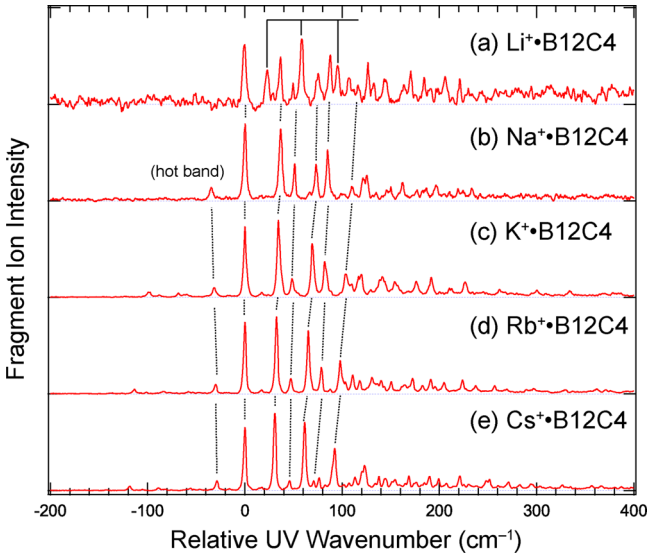

Figure 7. Expanded views of the UVPD spectra around the origin band.

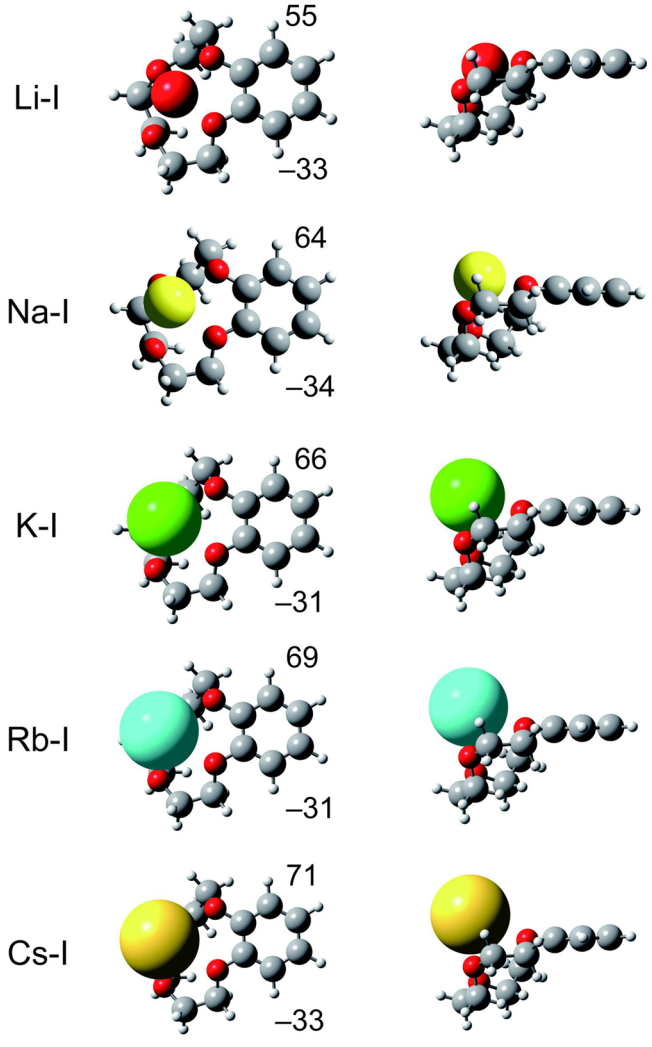

Figure 8. Most stable conformers of the M^+·B12C4 (M = Li, Na, K, Rb, and Cs) complexes calculated at the M05-2X/6-31+G(d) level of theory. The numbers in the figure represent the dihedral angle of C12−O1−C2−C13 and C5−O4−C3−C16 (Figure 1).

conformers in the UVPD spectra can be assigned to these forms in Figure 8.

The above assignment is confirmed by the TD-DFT calculations. Figure 9 shows the comparison of the UVPD

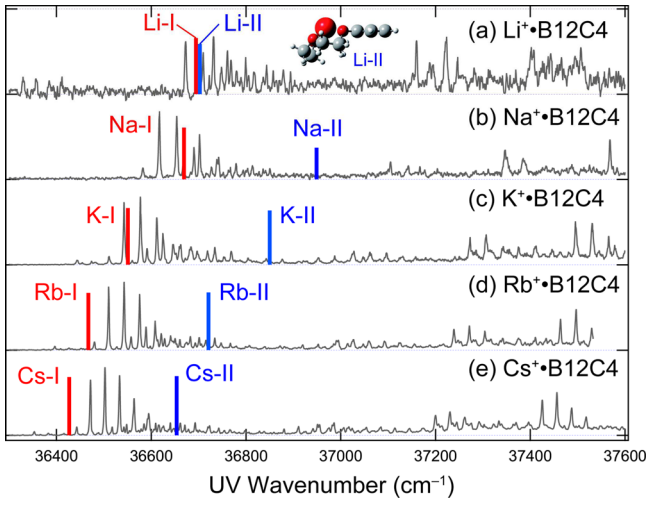

Figure 9. Comparison of the UVPD spectra and the TD-DFT results calculated at the M05-2X/6-31+G(d) level of theory. For the calculated transition energy, a scaling factor of 0.8340 is employed for the comparison. This factor is determined so as to simulate the transition energy of the K^+·DB18C6 complex in our previous study (ref 34). The structure of the second stable conformer of the Li^+ complex (Li-II) is displayed in the top panel.

spectra with the results of the TD-DFT calculations. The red and blue bars show the S_1-S_0 transition of the most and the second most stable conformers, respectively. The structure of the second most stable forms is shown in Figure S1 of the Supporting Information. These conformers seem to have a more flat structure in the B12C4 part than the most stable ones, and the distance between the metal ions and the benzene rings is shorter. The dihedral angles of these second conformers (Figure S1) are quite different from those of the most stable ones (Figure 8). As a result, the other part of the cavity also takes different forms from those of the most stable ones. For comparison of the UV spectra, a scaling factor of 0.8340 is employed for the calculated transition energy. This factor was independently determined so as to simulate the S_1-S_0 transition energy of the K^+·DB18C6 complex in our previous study,[34] and it was applicable to the M^+·B15C5 and M^+·B18C6 complexes very well.[35] For the Na^+·B12C4 to Cs^+·B12C4 complexes, the transition energy of the most stable conformers (red bars) is much closer to the origin band than that of the second ones (blue bars). Hence, the conformers in the experiments can be attributed to the most stable forms in Figure 8.

For the Li^+ complex, the transition energy of the most stable one (Li-I) well coincides with the origin band, but the transition energy of the second most stable one (Li-II, shown in Figure 9a) is close to that of the most stable one. Therefore, the other isomer found in the UVPD spectrum of the Li^+ complex (Figure 7a) can be ascribed to Li-II. The existence of two conformers for the Li^+·B12C4 complex seems to be probable because of a smaller difference in the total energy between the most and the second most stable structure (1.2 kJ/mol) among the M^+·B12C4 complexes. From the difference in the total energy, the relative abundance of Li-II to Li-I is estimated as 5

DOI: 10.1021/acs.jpca.6b06626
J. Phys. Chem. A 2016, 120, 6394−6401

$\times 10^{-7}$ at ~10 K. However, the vibronic bands of the second conformer are comparable to those of the first one as seen in Figure 7a. Hence, it is plausible that there is a potential barrier between Li-I and Li-II, and that Li-II is kinetically trapped in the cooling process.[34]

3.4. Relation between the Conformation of M^+·B12C4 and the Ion Selectivity of 12C4. The equilibrium constant for the complex formation between alkali metal ions and 12C4 was reported in methanol and propylene carbonate.[3,49] Though the absolute value of the constant is highly dependent on the solvent, 12C4 has the maximum value for Na^+ among alkali metal ions in both solvents.[3,49] Table 1 shows the number of conformers found under cold conditions in the gas phase.[35] In the case of the B15C5 and B18C6 complexes, these CEs have a flexibility to take different conformations for some metal ions. For the M^+·B12C4 complexes, there is one conformer for M = Na to Cs and two conformers for M = Li. Because the size of the crown ring of B12C4 is too small to have the conformation flexibility, the entropic advantage by taking different conformations cannot be obtained for any alkali metal ion in the M^+·B12C4 complexes.

Table 1. Number of Conformers for the M^+·B12C4, M^+·B15C5, and M^+·B18C6 (M = Li, Na, K, Rb, and Cs) Complexes

M	M^+·B12C4	M^+·B15C5[a]	M^+·B18C6[a]
Li	2	2	2
Na	1	1	3
K	1	3	2
Rb	1	3	1
Cs	1	3	1

[a]Reference 35.

As described above, the conformations in the B12C4 part are similar for all the M^+·B12C4 complexes. Figure 10 displays the distance between the metal ion and the mean plane formed with the oxygen atoms for the M^+·B12C4 (red), M^+·B15C5 (blue), and M^+·B18C6 (black) complexes. For the M^+·B15C5 and M^+·B18C6 complexes, the data are taken from our previous paper, and averaged values are plotted in Figure 10 if there are a few isomers for one complex.[35] The distance of the B15C5 complexes is almost zero for Li^+ and Na^+, but it becomes quite large for K^+ to Cs^+. In the case of the B18C6 complexes, the distance is close to zero for Li^+ to K^+, and it becomes larger than 0.5 Å for Rb^+ and Cs^+. These results are quite reasonable from the fact that B15C5 and B18C6 have an optimum matching in size with Na^+ and K^+, respectively, and hold these metal ions selectively among alkali metal ions in solution.[3,49] In contrast, the distance of the M^+·B12C4 complexes is larger than 0.5 Å for all the metal ions and increases monotonously with increasing ion radius, indicating that the cavity of B12C4 is too small even for Li^+ ion.

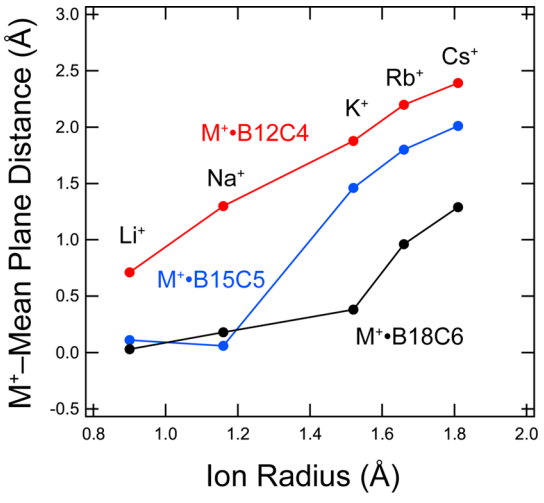

Figure 10. Distance between the metal ion and the mean plane formed with the oxygen atoms for M^+·B12C4 (red), M^+·B15C5 (blue), and M^+·B18C6 (black). The data of the M^+·B15C5 and M^+·B18C6 complexes are taken from our previous paper (ref 35).

In the case of the M^+·DB18C6 (M^+ = K^+, Rb^+, and Cs^+) complexes, the complex structure or the position of the metal ions against the crown part strongly affects the solvation manner, leading to the difference in the number of conformations for solvated systems, which can be related to the selectivity in solution.[37] Because the K^+·DB18C6 complex has the K^+ ion almost in the plane of the cavity, solvent molecules can be bonded to K^+·DB18C6 from both the top and bottom of the cavity, which gives multiple conformers. In contrast, the Rb^+ and Cs^+ ions in the DB18C6 complexes are located largely out of the DB18C6 cavity, and the solvent molecules can be bound only from the top of the complexes, showing only one stable conformer each.[37] A similar trend of the conformation for solvated systems is seen in the case of M^{2+}·B15C5 and M^{2+}·B18C6 (M = Ca, Sr, Ba, and Mn) complexes.[38] As shown in Figure 8, the M^+·B12C4 complexes have more or less the same structure; the metal ions cannot enter the crown cavity and are located on it. Therefore, the solvation manner to the M^+·B12C4 complexes in solution may be similar for all the alkali metal ions. Hence, the Na^+ preference of 12C4 among alkali metal ions in solution may originate mainly from the solvation of free metal ions, not from the solvation of the M^+·12C4 complexes. Compared with Na^+, Li^+ ion has larger solvation energy in solution, which results in a smaller change of Gibbs free energy and a smaller equilibrium constant in the course of the complex formation than the Na^+ case. Further investigation of the solvent effect to the ion selectivity of CEs by using microsolvation systems in the gas phase is also our future work.

4. SUMMARY

The UVPD spectra of the M^+·B12C4 (M = Li, Na, K, Rb, and Cs) complexes have been measured in the 36300−37600 cm^{-1} region. All the M^+·B12C4 complexes show sharp vibronic bands in this region. The UV−UV HB spectra have been measured for the Na^+ to Cs^+ complexes, and only one conformer was found for each complex, whereas the Li^+ complex has two conformers. The vibronic structures around the origin band of the UVPD spectra are quite similar for all the complexes, indicating the similarity of the complex structures. The most stable structures calculated also have similar structures among them, which coincides with the similarity of the vibronic structures in the UVPD spectra. In these conformers the metal ions are too big to enter the cavity of B12C4, even for the Li^+ ion. In solution, 12C4 shows the preference to Na^+ ion among alkali metal ions. On the basis of the similar structures of the M^+·B12C4 complexes, the selectivity of Na^+ ion in solution can be ascribed mainly to the solvation of free ions, not to the solvation of the M^+·12C4 complexes.

DOI: 10.1021/acs.jpca.6b06626
J. Phys. Chem. A 2016, 120, 6394−6401

■ ASSOCIATED CONTENT

Supporting Information

The Supporting Information is available free of charge on the ACS Publications website at DOI: 10.1021/acs.jpca.6b06626.

Structures of the second most stable conformers for the M^+·B12C4 (M = Li, Na, K, Rb, and Cs) complexes and full list of authors of ref 47 (PDF)

■ AUTHOR INFORMATION

Corresponding Author

*Y. Inokuchi. E-mail: y-inokuchi@hiroshima-u.ac.jp. Phone: +81 (Japan)-82-424-7101.

Notes

The authors declare no competing financial interest.

■ ACKNOWLEDGMENTS

This work was partly supported by JSPS KAKENHI Grant Number 16H04098.

■ REFERENCES

(1) Pedersen, C. J. Cyclic Polyethers and Their Complexes with Metal Salts. *J. Am. Chem. Soc.* **1967**, *89*, 7017−7036.

(2) Pedersen, C. J. The Discovery of Crown Ethers. *Science* **1988**, *241*, 536−540.

(3) Izatt, R. M.; Bradshaw, J. S.; Nielsen, S. A.; Lamb, J. D.; Christensen, J. J. Thermodynamic and Kinetic Data for Cation Macrocycle Interaction. *Chem. Rev.* **1985**, *85*, 271−339.

(4) Allen, F. H. The Cambridge Structural Database: A Quarter of a Million Crystal Structures and Rising. *Acta Crystallogr., Sect. B: Struct. Sci.* **2002**, *58*, 380−388.

(5) Diao, K.-S.; Wang, H.-J.; Qiu, Z.-M. A DFT Study on the Metal Binding Selectivity of 12-Crown-4 and Its Heterocyclic Analogs. *J. Mol. Struct.: THEOCHEM* **2009**, *901*, 157−162.

(6) Kim, H. S. Selectivity of between K^+ and Na^+ Ions to 12-Crown-4: Qspr Analysis by a Monte Carlo Simulation Study. *Bull. Korean Chem. Soc.* **2008**, *29*, 431−437.

(7) Zhang, H.; Chu, J. H.; Leming, S.; Dearden, D. V. Gas-Phase Molecular Recognition - Gas-Phase Crown-Ether Alkali-Metal Ion Complexes and Their Reactions with Neutral Crowns. *J. Am. Chem. Soc.* **1991**, *113*, 7415−7417.

(8) Maleknia, S.; Brodbelt, J. Gas-Phase Selectivities of Crown Ethers for Alkali-Metal Ion Complexation. *J. Am. Chem. Soc.* **1992**, *114*, 4295−4298.

(9) Ray, D.; Feller, D.; More, M. B.; Glendening, E. D.; Armentrout, P. B. Cation-Ether Complexes in the Gas Phase: Bond Dissociation Energies and Equilibrium Structures of Li^+(1,2-Dimethoxyethane)$_X$, X = 1 and 2, and Li^+(12-Crown-4). *J. Phys. Chem.* **1996**, *100*, 16116−16125.

(10) Armentrout, P. B.; Austin, C. A.; Rodgers, M. T. Alkali Metal Cation Interactions with 12-Crown-4 in the Gas Phase: Revisited. *Int. J. Mass Spectrom.* **2012**, *330*, 16−26.

(11) Armentrout, P. B.; Austin, C. A.; Rodgers, M. T. Alkali Metal Cation Interactions with 15-Crown-5 in the Gas Phase: Revisited. *J. Phys. Chem. A* **2014**, *118*, 8088−8097.

(12) Shubert, V. A.; James, W. H.; Zwier, T. S. Jet-Cooled Electronic and Vibrational Spectroscopy of Crown Ethers: Benzo-15-Crown-5 Ether and 4′-Amino-Benzo-15-Crown-5 Ether. *J. Phys. Chem. A* **2009**, *113*, 8055−8066.

(13) Shubert, V. A.; Muller, C. W.; Zwier, T. S. Water's Role in Reshaping a Macrocycle's Binding Pocket: Infrared and Ultraviolet Spectroscopy of Benzo-15-Crown-5-$(H_2O)_n$ and 4′-Aminobenzo-15-Crown-5-$(H_2O)_n$, n = 1, 2. *J. Phys. Chem. A* **2009**, *113*, 8067−8079.

(14) Kusaka, R.; Inokuchi, Y.; Ebata, T. Laser Spectroscopic Study on the Conformations and the Hydrated Structures of Benzo-18-Crown-6-Ether and Dibenzo-18-Crown-6-Ether in Supersonic Jets. *Phys. Chem. Chem. Phys.* **2007**, *9*, 4452−4459.

(15) Kusaka, R.; Inokuchi, Y.; Ebata, T. Structure of Hydrated Clusters of Dibenzo-18-Crown-6-Ether in a Supersonic Jet-Encapsulation of Water Molecules in the Crown Cavity. *Phys. Chem. Chem. Phys.* **2008**, *10*, 6238−6244.

(16) Kusaka, R.; Inokuchi, Y.; Ebata, T. Water-Mediated Conformer Optimization in Benzo-18-Crown-6-Ether/Water System. *Phys. Chem. Chem. Phys.* **2009**, *11*, 9132−9140.

(17) Kokubu, S.; Kusaka, R.; Inokuchi, Y.; Haino, T.; Ebata, T. Laser Spectroscopic Study on (Dibenzo-24-Crown-8-Ether)-Water and -Methanol Complexes in Supersonic Jets. *Phys. Chem. Chem. Phys.* **2010**, *12*, 3559−3565.

(18) Kusaka, R.; Kokubu, S.; Inokuchi, Y.; Haino, T.; Ebata, T. Structure of Host-Guest Complexes between Dibenzo-18-Crown-6 and Water, Ammonia, Methanol, and Acetylene: Evidence of Molecular Recognition on the Complexation. *Phys. Chem. Chem. Phys.* **2011**, *13*, 6827−6836.

(19) Inokuchi, Y.; Kusaka, R.; Ebata, T.; Boyarkin, O. V.; Rizzo, T. R. Laser Spectroscopic Study of Cold Host-Guest Complexes of Crown Ethers in the Gas Phase. *ChemPhysChem* **2013**, *14*, 649−660.

(20) Kusaka, R.; Inokuchi, Y.; Haino, T.; Ebata, T. Structures of (3*n*-Crown-*n*)-Phenol (n = 4, 5, 6, 8) Host-Guest Complexes: Formation of a Uniquely Stable Complex for n = 6 via Collective Intermolecular Interaction. *J. Phys. Chem. Lett.* **2012**, *3*, 1414−1420.

(21) Morishima, F.; Kusaka, R.; Inokuchi, Y.; Haino, T.; Ebata, T. Anomalous Cage Effect of the Excited State Dynamics of Catechol in the 18-Crown-6-Catechol Host-Guest Complex. *J. Phys. Chem. B* **2015**, *119*, 2557−2565.

(22) Rodriguez, J. D.; Lisy, J. M. Infrared Spectroscopy of Gas-Phase Hydrated K^+:18-Crown-6 Complexes: Evidence for High Energy Conformer Trapping Using the Argon Tagging Method. *Int. J. Mass Spectrom.* **2009**, *283*, 135−139.

(23) Rodriguez, J. D.; Lisy, J. M. Infrared Spectroscopy of Multiply Charged Metal Ions: Methanol-Solvated Divalent Manganese 18-Crown-6 Ether Systems. *J. Phys. Chem. A* **2009**, *113*, 6462−6467.

(24) Rodriguez, J. D.; Vaden, T. D.; Lisy, J. M. Infrared Spectroscopy of Ionophore-Model Systems: Hydrated Alkali Metal Ion 18-Crown-6 Ether Complexes. *J. Am. Chem. Soc.* **2009**, *131*, 17277−17285.

(25) Rodriguez, J. D.; Kim, D.; Tarakeshwar, P.; Lisy, J. M. Exploring Gas-Phase Ion-Ionophore Interactions: Infrared Spectroscopy of Argon-Tagged Alkali Ion-Crown Ether Complexes. *J. Phys. Chem. A* **2010**, *114*, 1514−1520.

(26) Martinez-Haya, B.; Hurtado, P.; Hortal, A. R.; Steill, J. D.; Oomens, J.; Merkling, P. J. Spectroscopic Investigation of the Gas-Phase Conformations of 15-Crown-5 Ether Complexes with K^+. *J. Phys. Chem. A* **2009**, *113*, 7748−7752.

(27) Martinez-Haya, B.; Hurtado, P.; Hortal, A. R.; Hamad, S.; Steill, J. D.; Oomens, J. Emergence of Symmetry and Chirality in Crown Ether Complexes with Alkali Metal Cations. *J. Phys. Chem. A* **2010**, *114*, 7048−7054.

(28) Hurtado, P.; Hortal, A. R.; Gámez, F.; Hamad, S.; Martínez-Haya, B. Gas−Phase Complexes of Cyclic and Linear Polyethers with Alkali Cations. *Phys. Chem. Chem. Phys.* **2010**, *12*, 13752.

(29) Kim, H. J.; Shin, W. J.; Choi, C. M.; Lee, J. H.; Kim, N. J. Electronic Photodepletion Spectroscopy of Dibenzo-18-Crown-6 with a Potassium Ion. *Bull. Korean Chem. Soc.* **2008**, *29*, 1973−1976.

(30) Choi, C. M.; Kim, H. J.; Lee, J. H.; Shin, W. J.; Yoon, T. O.; Kim, N. J.; Heo, J. Ultraviolet Photodepletion Spectroscopy of Dibenzo-18-Crown-6-Ether Complexes with Alkali Metal Cations. *J. Phys. Chem. A* **2009**, *113*, 8343−8350.

(31) Choi, C. M.; Lee, J. H.; Choi, Y. H.; Kim, H. J.; Kim, N. J.; Heo, J. Ultraviolet Photodepletion Spectroscopy of Dibenzo-18-Crown-6-Ether Complexes with Alkaline Earth Metal Divalent Cations. *J. Phys. Chem. A* **2010**, *114*, 11167−11174.

(32) Choi, C. M.; Choi, D. H.; Heo, J.; Kim, N. J.; Kim, S. K. Ultraviolet−Ultraviolet Hole Burning Spectroscopy in a Quadrupole Ion Trap: Dibenzo[18]Crown-6 Complexes with Alkali Metal Cations. *Angew. Chem., Int. Ed.* **2012**, *51*, 7297−7300.

(33) Choi, C. M.; Baek, J. Y.; Park, K. S.; Heo, J.; Kim, N. J. Conformation-Specific Ultraviolet Spectroscopy of Benzo-18-Crown-6

DOI: 10.1021/acs.jpca.6b06626
J. Phys. Chem. A 2016, 120, 6394−6401

Complexes with a Potassium Cation. *Chem. Phys. Lett.* **2014**, *593*, 150−153.
(34) Inokuchi, Y.; Boyarkin, O. V.; Kusaka, R.; Haino, T.; Ebata, T.; Rizzo, T. R. UV and IR Spectroscopic Studies of Cold Alkali Metal Ion-Crown Ether Complexes in the Gas Phase. *J. Am. Chem. Soc.* **2011**, *133*, 12256−12263.
(35) Inokuchi, Y.; Boyarkin, O. V.; Kusaka, R.; Haino, T.; Ebata, T.; Rizzo, T. R. Ion Selectivity of Crown Ethers Investigated by UV and IR Spectroscopy in a Cold Ion Trap. *J. Phys. Chem. A* **2012**, *116*, 4057−4068.
(36) Feraud, G.; Dedonder, C.; Jouvet, C.; Inokuchi, Y.; Haino, T.; Sekiya, R.; Ebata, T. Development of Ultraviolet-Ultraviolet Hole-Burning Spectroscopy for Cold Gas-Phase Ions. *J. Phys. Chem. Lett.* **2014**, *5*, 1236−1240.
(37) Inokuchi, Y.; Ebata, T.; Rizzo, T. R.; Boyarkin, O. V. Microhydration Effects on the Encapsulation of Potassium Ion by Dibenzo-18-Crown-6. *J. Am. Chem. Soc.* **2014**, *136*, 1815−1824.
(38) Inokuchi, Y.; Ebata, T.; Rizzo, T. R. Solvent Effects on the Encapsulation of Divalent Ions by Benzo-18-Crown-6 and Benzo-15-Crown-5. *J. Phys. Chem. A* **2015**, *119*, 8097−8105.
(39) Inokuchi, Y.; Ebata, T.; Rizzo, T. R. UV and IR Spectroscopy of Cold H_2O^+-Benzo-Crown Ether Complexes. *J. Phys. Chem. A* **2015**, *119*, 11113−11118.
(40) Inokuchi, Y.; Haino, T.; Sekiya, R.; Morishima, F.; Dedonder, C.; Feraud, G.; Jouvet, C.; Ebata, T. UV Photodissociation Spectroscopy of Cryogenically Cooled Gas Phase Host-Guest Complex Ions of Crown Ethers. *Phys. Chem. Chem. Phys.* **2015**, *17*, 25925−25934.
(41) Inokuchi, Y.; Soga, K.; Hirai, K.; Kida, M.; Morishima, F.; Ebata, T. Ultraviolet Photodissociation Spectroscopy of the Cold K^+.Calix-[4]Arene Complex in the Gas Phase. *J. Phys. Chem. A* **2015**, *119*, 8512−8518.
(42) Kang, H.; Féraud, G.; Dedonder-Lardeux, C.; Jouvet, C. New Method for Double-Resonance Spectroscopy in a Cold Quadrupole Ion Trap and Its Application to UV−UV Hole-Burning Spectroscopy of Protonated Adenine Dimer. *J. Phys. Chem. Lett.* **2014**, *5*, 2760−2764.
(43) Kobayashi, Y.; Inokuchi, Y.; Ebata, T. Ion Core Structure in $(CS_2)_n^+$ and $(CS_2)_n^-$ (n = 3−10) Studied by Infrared Photodissociation Spectroscopy. *J. Chem. Phys.* **2008**, *128*, 164319.
(44) Goto, H.; Osawa, E. Corner Flapping: A Simple and Fast Algorithm for Exhaustive Generation of Ring Conformations. *J. Am. Chem. Soc.* **1989**, *111*, 8950−8951.
(45) Goto, H.; Osawa, E. An Efficient Algorithm for Searching Low-Energy Conformers of Cyclic and Acyclic Molecules. *J. Chem. Soc., Perkin Trans. 2* **1993**, 187−198.
(46) Inokuchi, Y.; Ebata, T.; Ikeda, T.; Haino, T.; Kimura, T.; Guo, H.; Furutani, Y. New Insights into Metal Ion-Crown Ether Complexes Revealed by SEIRA Spectroscopy. *New J. Chem.* **2015**, *39*, 8673−8680.
(47) Frisch, M. J.; Trucks, G. W.; Schlegel, H. B.; Scuseria, G. E.; Robb, M. A.; Cheeseman, J. R.; Scalmani, G.; Barone, V.; Mennucci, B.; Petersson, G. A.; et al. *Gaussian 09*, Revision A.1; Gaussian, Inc.: Wallingford, CT, 2009.
(48) Schuchardt, K. L.; Didier, B. T.; Elsethagen, T.; Sun, L. S.; Gurumoorthi, V.; Chase, J.; Li, J.; Windus, T. L. Basis Set Exchange: A Community Database for Computational Sciences. *J. Chem. Inf. Model.* **2007**, *47*, 1045−1052.
(49) Chu, I. H.; Zhang, H.; Dearden, D. V. Macrocyclic Chemistry in the Gas-Phase - Intrinsic Cation Affinities and Complexation Rates for Alkali-Metal Cation Complexes of Crown-Ethers and Glymes. *J. Am. Chem. Soc.* **1993**, *115*, 5736−5744.

DOI: 10.1021/acs.jpca.6b06626
J. Phys. Chem. A 2016, 120, 6394−6401